Trans. Tianjin Univ. 2011, 17: 033-038
DOI 10.1007/s12209-011-1458-y

Simplification and Experimental Verification for Temperature and Humidity Field Coupling Model of Conservatory Soil

CAO Binbin（曹滨斌），LI Weiyi（李惟毅），LI Zhaoli（李兆力）
（School of Mechanical Engineering, Tianjin University, Tianjin 300072, China）

Abstract：Based on the surface energy balance model which is widely used abroad, a temperature and humidity field coupling model of conservatory soil without crop vegetation in full illumination was established. Considering the relatively closed environment in conservatory, weak solar radiation and little surface evaporation of soil, the daily variation of water content in different soil layers may be neglected, then the temperature and humidity field coupling model was simplified to a one-dimensional thermal diffusion model. The simplified model and the temperature and humidity field coupling model adopted the same computational method of soil physical parameters and discrete format of heat diffusion differential equations, and were applied to the continuous simulation of temperature field in conservatory soil without crop vegetation in full illumination. Through the comparison between simulation results and experimental data, the precision of the simplified model was verified. The typical rule of soil heat flux variation in a 24 h cycle was also obtained.

Keywords：conservatory; soil; temperature; humidity; coupling model; simplification

The important and direct source of heat requirement of conservatory in winter evenings comes from thermal storage of soil. The research on the distribution of heat and water content in conservatory soil is significant for grasping the rules of mass-energy exchange near the soil surface to condition a suitable circumstance for crop growth.

In recent years, the mechanism of thermal storage（or heat release）process in soil mainly based on temperature and humidity field coupling model have been studied by domestic and foreign scholars. Chen *et al*[1] carried out dynamic simulation of the temperature and humidity field in soil under solar radiation. Liu *et al* [2-4] made numerical calculation and experimental investigation on the heat and mass transfer in conservatory soil. Fan *et al*[5,6] calculated daily variation of soil temperature with heat-moisture-gas coupling model and carried out some experimental investigations. All these research results provided reference for the study of thermal storage to some extent. Owing to the multi-parameter and complex relations among the parameters in temperature and humidity field coupling model, it is difficult to work out the result, either in analytical solution or in numerical solution. Based on the previous research results and the widely used surface energy balance theoretical model, this paper establishes the temperature and humidity field coupling model of conservatory soil without crop vegetation in full illumination. The model is further simplified to a one-dimensional thermal diffusion model.

1 Mathematical model

1.1 Assumptions

（1）The existence of conservatory has no direct influence on outdoor weather parameters;

（2）Only shortwaves can transmit the covering material of conservatory, and the influence of the condensation of steam on the surface on transmissivity can be neglected;

（3）It is assumed that the direct solar radiation consisted of 50% visible light and 50% near infrared light, and the scattering part of solar radiation was all considered as visible light;

（4）According to the Kindelan’s conclusion, in large conservatory, one-dimensional heat transfer equation can be adopted to describe the heat transfer in soil.

Accepted date: 2009-12-01.
CAO Binbin, born in 1981, male, Dr.
Correspondence to CAO Binbin, E-mail: bttxw@yahoo.com.cn.

1.2 Temperature and humidity field coupling model

The main energy source of conservatory is from solar radiation. The energy balance on soil surface accords with the equation[7]:

$$R_n - H - LE - G = 0 \tag{1}$$

Each item in the equation will be described thereinafter. The equation can be translated into $R_n = H + LE + G$, which is the intuitive expression of surface energy balance model widely adopted by foreign scholars.

1.2.1 Net heat gain of soil surface

The net heat gain of soil surface from solar radiation R_n consists of shortwave and longwave radiations, which can be calculated by

$$R_n = (\tau_{\text{dir-cover}} R_{\text{dir}} + \tau_{\text{dif-cover}} R_{\text{dif}})(1-\rho_{\text{soil}}) + \sum \sigma \varepsilon_{i\text{-soil}} f_{i\text{-soil}} A_i (T_i^4 - T_{\text{soil}}^4) \tag{2}$$

where $\tau_{\text{dir-cover}}$ is direct solar transmissivity of conservatory material; R_{dir} the direct solar heat, W; $\tau_{\text{dif-cover}}$ diffusion solar transmissivity of conservatory material; R_{dif} diffusion solar heat, W; ρ_{soil} reflectivity of the soil surface; $\varepsilon_{i\text{-soil}}$ indoor blackness between each surface of wall and soil surface; $f_{i\text{-soil}}$ the angle coefficient of heat radiation between each surface of wall and soil surface; T_i and T_{soil} are temperatures of each surface of wall and soil surface, K.

1.2.2 Heat convection between conservatory soil surface and air

According to the relative closure of conservatory, the convective heat transfer between conservatory soil surface and air H can be calculated by the natural convective heat transfer correlation equation[8]:

$$Nu = \frac{Hl}{\lambda \Delta T} = 0.14 Ra^{1/3} = 0.14\left(\frac{l^3 g b \Delta T}{\nu^2} Pr\right)^{1/3} \tag{3}$$

H is independent of characteristic length l in Eq. (3).

1.2.3 Heat transfer caused by evaporation in soil

With abundant sunlight, continuous evaporation occurs in soil because of the humidity difference between the indoor air and soil surface, so the heat absorbed by indoor air LE is calculated by[9]

$$LE = 0.016\,8 f h_{\text{soil}}[(aT_{\text{soil}} + b) - r_a(aT_a + b)] \tag{4}$$

where L is latent heat of steam, kJ/kg; E evaporation rate of steam, kg/(m^2·s); h_{sur} convective heat transfer coefficient between the indoor air and soil surface, W/(m^2·K); T_a indoor air temperature, K; a = 103 Pa/K; b = 609 Pa; r_a relative humidity of the air above soil surface; f coefficient related to crop vegetation and soil water content.

According to mass conservation,

$$LE - LE_c = 0 \tag{5}$$

where LE_c is latent heat transfer caused by the water content variation in the time interval ∂t, which is represented as

$$LE_c = L\int_0^z \frac{\partial \theta}{\partial t} \mathrm{d}z \tag{6}$$

where θ is the volumetric water content in soil, kg/m^3. The expansion of $\partial\theta/\partial t$ in the depth direction is[7]

$$\partial\theta/\partial t = \partial(K_c \partial\psi/\partial z)/\partial z + \partial(gK_c)/\partial z + \partial(hsD_v \partial T/\partial z)/\partial z + \partial(e_v D_v \partial h/\partial z)/\partial z \tag{7}$$

The former two items on the right side of Eq. (7) describe soil-water movement in liquid state driven by water potential gradient and gravity field. The latter two items describe soil-water movement in vapor state driven by temperature and water potential gradient.

1.2.4 Heat conduction in soil

Similar to the analysis of evaporation latent heat, heat conduction in soil G is described as one-dimensional form in the depth direction:

$$G = \int_0^z C_s \frac{\partial T}{\partial t} \mathrm{d}z \tag{8}$$

where C_S is volumetric heat capacity of soil, $C_s = \sum \rho_i C_i V_i$ [10], J/(m^3·K). The expansion of Eq. (8) is[7]

$$C_s \partial T/\partial t = \partial(K_s \partial T/\partial z)/\partial z + \partial(hsLD_v \partial T/\partial z)/\partial z + \partial(e_v LD_v \partial h/\partial z)/\partial z \tag{9}$$

where K_S is the thermal conductivity of soil, $K_s = \frac{\sum \zeta_i K_i V_i}{\sum \zeta_i V_i}$ [11], W/(m·K). ξ_i, K_i are mass coefficient and thermal conductivity of each soil component respectively. The first item on the right side of Eq. (9) is heat flux driven by temperature gradient. The second item is energy flow induced by steam movement in soil with temperature gradient. The last item is energy flow caused by water potential gradient in soil.

1.3 Simplified one-dimensional thermal diffusion model

Considering that indoor humidity of conservatory in winter is large and the environmental radiation is relatively weak, the daily variation of soil humidity can be neglected and a simplified mathematical model is obtained.

As the conservatory is in full illumination, the length of each direction is much larger than the vertical depth of soil, so the research object can be considered as a semi-infinite body. Only the temperature variation of soil in depth direction needs to be considered. Thereby, for isotropic soil, Eq.(9) can be simplified to

$$C_s \partial T / \partial \tau = K_s \partial^2 T / \partial x^2 \tag{10}$$

where C_s and K_s are both the function of soil temperature and water content θ. In Eq.(10), the calculation accuracy of this model is dependent on the value of C_s and K_s.

2 Calculation of parameters

The selection of parameters directly determines the calculation accuracy of this model. These parameters are listed in Tab.1.

Tab.1 Calculation of parameters in the soil model

Parameter	Temperature and humidity coupling model	Description
The volumetric heat capacity of soil C_s [11]	$\rho_m C_m V_m + \rho_q C_q V_q + \rho_o C_o V_o + \rho_a C_a V_a + \rho_w C_w V_w$	ρ, C and V are density, heat capacity and volumetric fraction, respectively; subscripts " m,q,o,a and w " represent mineral, quartz, organic matter, air and water, respectively. V is related to soil type and water content in soil.
Thermal conductivity K_s [11]	$\dfrac{\xi_w K_w V_w + \xi_g K_g V_g + \xi_m K_m V_m}{\xi_w V_w + \xi_g V_g + \xi_m V_m}$	Subscripts " w,g and m " represent water, air and mineral in soil, respectively.
Hydraulic conductivity K_c [11]	$K_h(\theta/\theta_s)^{2b+3}$	K_h is saturated hydraulic conductivity of soil; θ_s volumetric water content of saturated soil; b constant related to soil structure. K_h and b of each kind of soil are given in Ref.[11].
Diffusion coefficient D_v [7]	$D_{av}(0.622\rho/P)[(\phi_a - m)/(1-m)]^n$	m and n are empirical constants presented by Toeh *et al*, $m = 0.05$, $n = 1.5$.
Water potential ψ [7]	$\psi_0(\theta/\theta_s)^{-b_1}$	ψ_0 is water potential of saturated soil related to soil type, the value range is usually 0.6—9; b_1 is an empirical constant related to soil structure, the value range is usually 2—24.
Relative humidity h [7]	$\exp(\psi_0(\theta/\theta_s)^{-b_1}/RT_s)$	
Saturated vapor pressure s [11]	$\dfrac{bce_s(T)}{(c+T)^2}$	The calculation of e_s and values of b and c are given in Ref.[11].

3 Discretization of differential equation

Numerical investigation was carried out on 50 cm deep conservatory soil without crop vegetation in full illumination. Numerical meshes were generated with 2 cm interval in depth direction and 1 min time interval as shown in Fig.1. The equations of the two models mentioned above were discretized respectively. Iteration scheme of Crank-Nicolson was adopted with the node division shown in Fig.1.

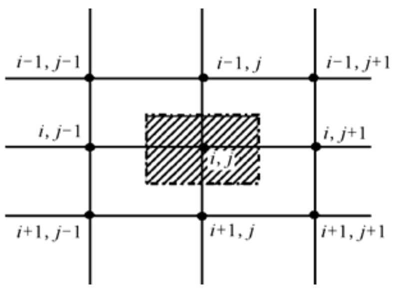

Fig.1 Sketch map of node division

Before discretization, the temperature and humidity field coupling model is simplified to

$$C_h \partial h / \partial t = \partial(K_a \partial T_s / \partial z) + \partial(K_b \partial h / \partial z)/\partial z + g\partial K_c / \partial z \tag{11}$$

$$C_s \partial T_s / \partial t = \partial(K_d \partial T_s / \partial z)/\partial z + \partial(K_e \partial h / \partial z)/\partial z \tag{12}$$

The discretization of Eq.(11) is

$$\begin{aligned} & C_{h_i+1/2,j}(h_{i,j+1} - h_{i,j})/\delta\tau = \\ & \{K_{a_i+1/2,j}[(T_{s_i+1,j+1} - T_{s_i,j+1}) + (T_{s_i+1,j} - T_{s_i,j})] - \\ & K_{a_i-1/2,j}[(T_{s_i,j+1} - T_{s_i-1,j+1}) + (T_{s_i,j} - T_{s_i-1,j})] + \\ & K_{b_i+1/2,j}[(h_{i+1,j+1} - h_{i,j+1}) + (h_{i+1,j} - h_{i,j})] - \\ & K_{b_i-1/2,j}[(h_{i,j+1} - h_{i-1,j+1}) + (h_{i,j} - h_{i-1,j})]\}/2\delta z^2 + \\ & g(K_{c_i+1,j} - K_{c_i,j})/\partial z \quad i = 0,1,2,\cdots,25 \end{aligned} \tag{13}$$

Similarly, the discretization of Eq.(12) is

$$\begin{aligned} & C_{s_i+1/2,j}(T_{i,j+1} - T_{i,j})/\delta\tau = \\ & \{K_{d_i+1/2,j}[(T_{s_i+1,j+1} - T_{s_i,j+1}) + (T_{s_i+1,j} - T_{s_i,j})] - \\ & K_{d_i-1/2,j}[(T_{s_i,j+1} - T_{s_i-1,j+1}) + (T_{s_i,j} - T_{s_i-1,j})] + \\ & K_{e_i+1/2,j}[(h_{i+1,j+1} - h_{i,j+1}) + (h_{i+1,j} - h_{i,j})] - \\ & K_{e_i-1/2,j}[(h_{i,j+1} - h_{i-1,j+1}) + (h_{i,j} - h_{i-1,j})]\}/2\delta z^2 \\ & i = 0,1,2,\cdots,25 \end{aligned} \tag{14}$$

The discretization of simplified model is

$$\begin{aligned} & C_{s_i+1/2,j}(T_{i,j+1} - T_{i,j})/\delta\tau = K_{s_i+1/2,j}[(T_{i+1,j+1} - T_{i,j+1}) + \\ & (T_{i+1,j} - T_{i,j})] - K_{s_i-1/2,j}[(T_{i,j+1} - T_{i-1,j+1}) + \\ & (T_{i,j} - T_{i-1,j})]/2\delta x^2 \quad i = 1,2,\cdots,24 \end{aligned} \tag{15}$$

where i and j represent the space node and time node respectively. The temperature distribution at any time can be continuously simulated by Eq.(13)—Eq.(15) when initial conditions and boundary conditions are given. At the same time, according to temperature data, heat flux of different soil layers at any time can be worked out after discretizing Fourier Law:

$$q = -K_s \cdot \frac{\partial t}{\partial x}$$

4 Establishment of initial and boundary conditions

4.1 Heat-moisture coupling model

(1) Upper boundary

Temperature is given as the first boundary condition:

$$T_{soil}(0, j) = T_{soil}(\tau)$$

Water content $\theta(0, j)$ is given in the following step: evaporation of surface water is equal to water variation in soil, i.e.,

$$LE_s = LE_c = r_{sL} \cdot \sum_{i=0}^{25} \frac{\theta(i, j+1) - \theta(i, j)}{\delta\tau} =$$

$$r_{sL} \cdot \sum_{i=0}^{25} \frac{\theta(i, j+1) - \theta(i, j)}{60}$$

where r_{sL} is latent heat of steam at soil temperature, kJ/kg.

Setting $f(\theta(0, j)) = LE_s(\theta(0, j)) - LE_c(\theta(0, j))$, Newton iteration was adopted to solve $\theta(0, j)$ at any time.

(2) Lower boundary

The 50 cm deep soil is considered as constant temperature and constant humidity:

$$\frac{\partial T_{soil}}{\partial z} = 0, \frac{\partial \theta}{\partial z} = 0 \text{ or}$$

$$T_{soil}(25, j) = T_{soil\,n} = \text{const}, \theta(25, j) = \theta_n = \text{const}, z = z_0$$

4.2 Simplified model

(1) Initial condition

$$\tau = 0, \ t = t(i, j = 0), \ \theta = \theta(i, j = 0)$$

(2) Boundary condition

Upper boundary: $x = 0, t = t(0, \tau)$

Lower boundary: $\frac{\partial t}{\partial x} = 0, \ \frac{\partial \theta}{\partial x} = 0$ or

$$t(n, j) = t_n = \text{const}, \ \theta(n, j) = \theta_n = \text{const}$$

5 Numerical simulation and experimental verification

The experiment was carried out in a modern agricultural demonstration zone in Tianjin, on January 11, 2003. The three-span experimental conservatory with a total area of 9 576 m^2 is of Venlo type and enveloped by glass. The heating system consisted of coil filled with geothermal water, and worked from 16:00 to 9:00 next day. After selecting a piece of conservatory soil in western span without crop vegetation, the temperature and humidity distribution at initial time was recorded through collecting soil samples. The soil temperatures with 2 h time interval during 24 h were recorded continuously by EN880 Automatic Recorder. Simultaneously, numerical simulation was conducted using the above two models respectively. Temperature comparisons between experiment and numerical simulation value are shown in Fig.2—Fig.4 respectively, indicating the results at 10 cm, 20 cm, 40 cm depth in soil.

As shown in Fig.2—Fig.4, the variation trends are reflected in both models, the biggest error of the temperature and humidity field coupling model is around 15%, while that of the simplified model is 4.85%. The errors comes from the deviation in measured values of the soil surface temperature which is the boundary condition in numerical simulation and affects simulation precision greatly. Moreover, every soil parameter has an instant effect on soil temperature field during simulation, while there exists a delay in reality.

Fig.2—Fig.4 also show that the simplified model achieves a higher precision. Two main factors result in precision difference between the simplified model and coupling model. Firstly, the parameters used in the coupling model were almost determined by users' experience. Secondly, as more parameters were adopted in the coupling model, more error components exist in the result of coupling model, the comprehensive error would be amplified step by step. So a higher precision has been obtained in the simplified model due to its fewer parameters. Meanwhile, the simplified model can meet requirement when testing condition was limited or only common precision was needed in engineering practice.

Fig.5 shows the temperature variation of different depths in soil according to the experimental data. Tab.2 lists the heat flux of different depths in soil at different moments, which was calculated by the simplified model. According to Fig.5 and Tab.2, the daily heat storage and release rule in soil is obtained as follows: (1) The surface heat flux reaches the maximum of the day at about 12:00 due to solar radiation, it changes into a negative value at about 16:00 due to the reduction and disappearance of solar radiation, but the deep soil is still in the state of heat storage till 20:00 when the surface heat flux becomes

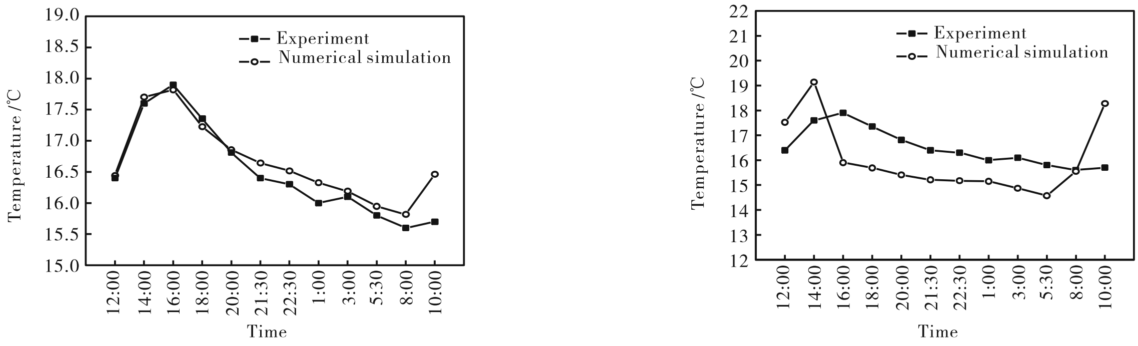

(a) Simplified model (b) Coupling model

Fig.2 Temperature comparison between simulation and experiment at 10 cm depth in soil

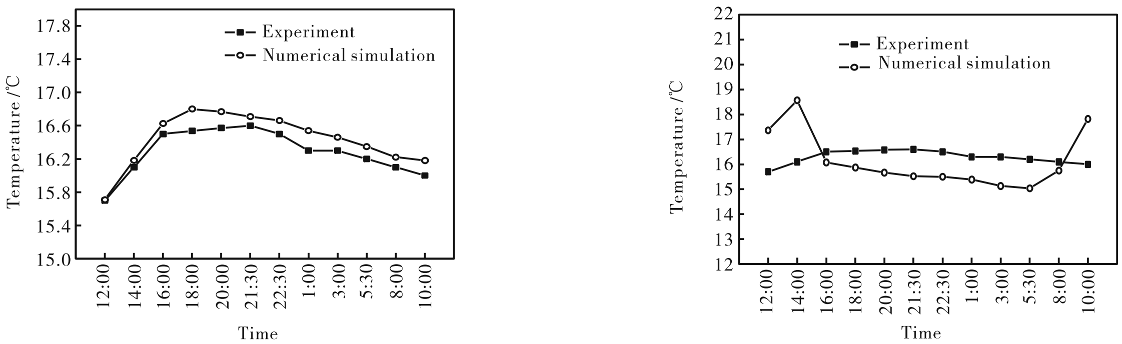

(a) Simplified model (b) Coupling model

Fig.3 Temperature comparison between simulation and experiment at 20 cm depth in soil

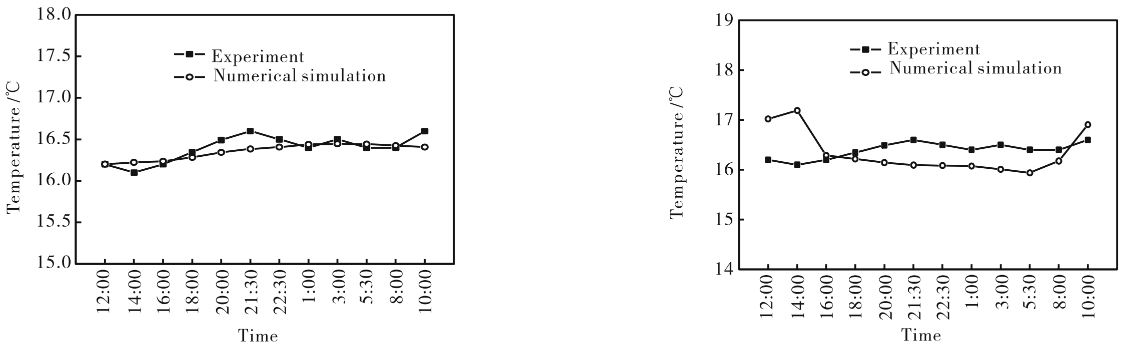

(a) Simplified model (b) Coupling model

Fig.4 Temperature comparison between simulation and experiment at 40 cm depth in soil

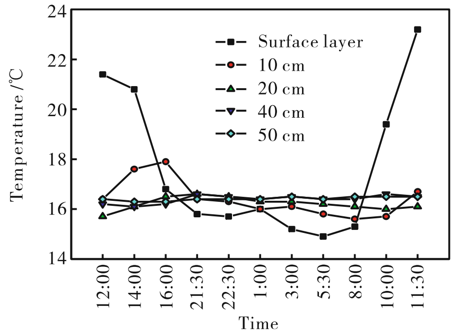

Fig.5 Temperature-time curve of different depths in soil

negative and the heat flux of different depths in soil all changes into the state of heat release, which would keep all night till 8:00 in the next morning. Subsequently, due to the enhancement of solar radiation, the surface heat flux becomes positive and continuously increases, deep soil begins to store heat in turn. (2) There is time delay in sequence among the moment when each layer heat flux inflection occurs. The influence of solar radiation on deep soil is small. (3) With the increase of soil depth, heat flux decreases in sequence, the heat flux at 40 cm

Tab.2 Heat flux of different depths in soil at different moments during one day

Depth/cm	Heat flux / ($W \cdot m^{-2}$)								
	12:00	16:00	18:00	20:00	0:00	4:00	6:00	8:00	10:00
0	44.48	−28.11	−10.67	−9.34	−4.00	−10.03	−6.96	12.77	50.96
10 cm	11.90	10.37	1.06	−1.39	−2.98	−3.98	−5.05	−3.77	4.29
20 cm	−3.03	6.51	4.93	2.67	−5.82	−1.09	−1.71	−2.22	−1.61
40 cm	−1.68	−1.30	−0.72	−0.11	0.45	0.41	0.30	0.14	−0.06

Note: the downwards heat flux is positive.

depth in soil tends to be constant during the day, the depth of 50 cm is considered as constant temperature strata. In addition, Tab.2 also shows that the surface heat flux is smaller in the evening, which is yielded by the ground heating coil in the conservatory.

6 Conclusions

(1) The temperature and humidity field coupling model of conservatory soil without crop vegetation in full illumination is simplified into a one-dimensional thermal diffusion model, which is proved to achieve good precision through comparison between simulation results and experimental data.

(2) The simplified model is applicable to limited test condition with common precision requirement.

(3) The heat flux of soil surface in conservatory reaches the maximum approximately at noon.

(4) The conservatory soil is in the state of heat release from 20:00 to 8:00 in the next morning.

(5) The moment when heat flux of each layer changes delays in sequence, and solar radiation has less influence on deep soil.

(6) There is almost no temperature fluctuation in conservatory with heat supply. The depth of 50 cm can be considered as constant temperature strata.

References

[1] Chen Zhenqian, Shi Mingheng. Simulation of temperature and moisture distribution in unsaturated soil under exposure of solar radiation[J]. *Acta Energiae Solaris Sinica*, 1998(1): 13-19 (in Chinese).

[2] Chen Wei, Liu Wei, Huang Suyi. A study of convective heat transfer in passive solar conservatory with storage[J]. *Journal of Engineering Thermophysics*, 2003, 24(3): 508-510 (in Chinese).

[3] Liu Bingcheng, Liu Wei, Wang Chongqi. Study on heat and mass migration and water evaporation in soil with dry surface layer under natural environment conditions[J]. *Acta Energiae Solaris Sinica*, 2004, 25(3): 299-304 (in Chinese).

[4] Fan Aiwu, Liu Wei, Li Guangzheng. Modeling for simultaneous transfer of heat, moisture, gas and solute in soil with plants growing[J]. *Journal of Huazhong University of Science and Technology*, 2005, 33(9): 59-61 (in Chinese).

[5] Fan Aiwu, Liu Wei, Wang Chongqi. Simulation on the daily change of soil temperature under various environment conditions [J]. *Acta Energiae Solaris Sinica*, 2003, 24(2): 167-171 (in Chinese).

[6] Fan Aiwu, Liu Wei, Wang Chongqi. Experimental study on the daily changes of soil temperature and water content[J]. *Acta Energiae Solaris Sinica*, 2002, 23(6): 721-724 (in Chinese).

[7] Qin Zhihao, Berliner Pedro, Karnieli Arnon. Numerical solution of a complete surface energy balance model for simulation of heat fluxes and surface temperature under bare soil environment[J]. *Applied Mathematics and Computation*, 2002, 130(1): 171-200.

[8] Jacobs A F G, Verhoef A. Soil evaporation from sparse natural vegetation estimated from Sherwood numbers[J]. *Journal of Hydrology*, 1997, 188-189: 443-452.

[9] Mihalakakou G. On estimating soil surface temperature profiles[J]. *Energy and Buildings*, 2002, 34(3): 251-259.

[10] Lei Zhidong, Yang Shixiu, Xie Senchuan. *Soil Hydrodynamic*[M]. Tsinghua University Press, Beijing, China, 1988 (in Chinese).

[11] Campbell G S, Norman J M. *An Introduction to Environmental Biophysics*[M]. Springer, New York, USA, 1998. 119-121.